American Journal of BioScience
2023; 11(2): 46-56
http://www.sciencepublishinggroup.com/j/ajbio
doi: 10.11648/j.ajbio.20231102.12
ISSN: 2330-0159 (Print); ISSN: 2330-0167 (Online)

Computational Exploration of *Vitis vinifera*-Derived Molecules as SARS-CoV-2 Main Protease Inhibitors: A Quantum Chemical and Molecular Modeling Approach

Owolabi Mutolib Bankole

Department of Chemical Sciences, Adekunle Ajasin University, Akungba, Nigeria

Email address:
owolabi.bankole@aaua.edu.ng

To cite this article:
Owolabi Mutolib Bankole. Computational Exploration of *Vitis Vinifera*-Derived Molecules as SARS-CoV-2 Main Protease Inhibitors: A Quantum Chemical and Molecular Modeling Approach. *American Journal of BioScience.* Vol. 11, No. 2, 2023, pp. 46-56.
doi: 10.11648/j.ajbio.20231102.12

Received: May 17, 2023; **Accepted**: June 2, 2023; **Published**: June 9, 2023

Abstract: The COVID-19 pandemic, caused by the SARS-CoV-2 virus, has unleashed a global health crisis, resulting in an alarming number of cases exceeding 765 million and deaths surpassing 6 million as of March 2023. Consequently, researchers worldwide are dedicating their efforts to exploring potential drug candidates that can serve as effective therapeutic interventions against this devastating virus. Meanwhile, the popularity of herbal medicines is skyrocketing, as individuals increasingly seek alternative remedies to address various health concerns within different healthcare systems around the world. In this study, a multitude of computational tools were employed to meticulously investigate the Vitis Vinifera extracts for their potential as inhibitors of the SARS-CoV-2 Mpro enzyme. These tools encompassed molecular docking, binding energy calculation, ADMET studies as well as quantum chemical calculations. The objective was to identify specific compounds present in Vitis Vinifera extracts that could effectively hinder the activity of the SARS-CoV-2 Mpro enzyme, a crucial target for therapeutic intervention. The rigorous analysis conducted unveiled six compounds that demonstrated significant potential as inhibitors of the SARS-CoV-2 Mpro enzyme: Hyperoside, Gallocatechin gallate, cis-Astringin, peonidin-3-O-glucoside, Fraxin, and cis-Piceid. When compared to the established standard drug Nelfinavir, these compounds exhibited superior binding affinities and slightly improved ADMET properties. Notably, peonidin-3-O-glucoside emerged as an especially promising compound, surpassing the others as well as the standard drug in terms of binding energy, reactivity, and stability. These findings suggest its potential as a potent inhibitor of the SARS-CoV-2 Mpro enzyme. However, it is imperative to emphasize that further validation through in vivo and in vitro studies is indispensable. While the computational results provide valuable insights, their practical application necessitates verifying the efficacy and safety of these compounds.

Keywords: SARS-CoV-2 Mpro, *Vitis Vinifera*, Molecular Docking, Binding Energy Calculation, Admet, Quantum Chemical Calculations

1. Introduction

The emergence of the COVID-19 pandemic caused by the SARS-CoV-2 virus has led to unparalleled health and economic crises worldwide with more than 765 million cases and 6 million deaths as of March 2023 [1, 2]. The primary mode of transmission for the virus is through respiratory droplets, and its symptoms can vary from mild to severe [3]. These symptoms encompass a range of conditions, including pneumonia and acute respiratory distress syndrome, which can be fatal in severe instances [4].

The outbreak of COVID-19 has posed a significant difficulty for governments, individuals, and society in general. It has affected various aspects of our lives such as health, economy, education, and social interactions [5, 6].

The main protease (Mpro) or 3C-like protease (3CLpro) is a crucial component in the replication of SARS-CoV-2, and it represents a potential drug discovery target, as Mpro plays a significant role in the production of non-structural proteins required for the virus to replicate, as it cleaves viral polyproteins [7, 8]. Therefore, it is an appealing target for drug development. Many researchers are focusing on

developing Mpro inhibitors to combat COVID-19 [7-9].

There is promising and reassuring evidence that the identification and development of compounds from natural sources, specifically plants, can lead to potential drug candidates that could be used as therapeutic interventions against viral diseases including COVID-19 [10].

Grapevine, scientifically known as *Vitis Vinifera*, is a readily available natural source of compounds that have potential pharmacological benefits [11]. Earlier research has established the presence of different phytochemicals, including flavonoids, stilbenes, and phenolic acids, in extracts from *V. Vinifera* [12]. Some of these compounds have exhibited antiviral properties against various diseases, including SARS-CoV [13].

Molecular modeling is a computational method that allows the prediction of ligand-receptor interactions and drug efficacy before synthesis or testing in vitro [14]. The use of molecular modeling has increased in recent years due to its speed, cost-effectiveness, and the ability to provide valuable insights into drug design [15].

In this research, we aim to study the molecule modeling of SARS-CoV-2 Mpro inhibitors from *V. Vinifera* extracts. Specifically, molecular docking, binding energy calculation, Absorption, Distribution, Metabolism, Excretion, and Toxicity (ADMET) study and quantum chemical calculations was employed to predict the binding affinities and stability of the identified compounds with the Mpro active site.

In this research, a library of compounds from *V. Vinifera* was screened against the Mpro active site using various tools from the Schrodinger Suite. The outcome of this study can offer valuable understanding of the molecular interactions between the phytochemicals present in *V. Vinifera* and the SARS-CoV-2 Mpro. This, in turn, could lead to the discovery of novel and effective Mpro inhibitors with potential therapeutic applications against COVID-19. The findings could also serve as a foundation for further exploration of other potential natural sources that may contain compounds with anti-SARS-CoV-2 properties.

2. Materials and Methods

2.1. Molecular Modeling

To investigate potential inhibitors of SARS-CoV-2 main protease, the Glide module [16] of Schrodinger software was used to perform the docking studies, using a database of compounds that were identified with V. vinifera. The ligands used in the docking studies were prepared by downloading their 2D structures from an online database (PubChem) [17], and then using the LigPrep tool [18] of the Schrodinger suite to convert them into 3D structures. The crystal structure of SARS-CoV-2 Main Protease (PDB ID: 7VLO) was retrieved from an online database (RCSB) [19], and prepared using the protein preparation wizard tool of the Schrodinger suite to fix any errors that may have been associated with the protein during crystallization.

The protein preparation process involved the addition of hydrogen, assigning bond orders, creating di-sulphide bridges, deleting water, optimization at pH 7.0, and minimization using the OPLS3e force field [20]. A cubic box was generated around the active site of the protein to map out the region where the ligand and the receptor interact. The grid was generated by selecting the complexed ligand which provides insight into the active site.

The molecular docking algorithm was performed using the glide tool of the Schrodinger suite [21]. The prepared ligands were docked using the Standard Precision (SP) and Extra Precision (XP) docking algorithms of the glide tool [16]. A standard drug was also docked using the same procedure to generate a comparative study between the lead compounds and the standard.

2.2. ADMET Screening

The lead compounds obtained from the molecular docking were further subjected to ADMET screening using the swissADME and Pro-tox II servers [22, 23]. These tests were performed to generate the physiochemical properties, pharmacokinetic profile, drug-likeness, and toxicity of the lead compounds.

2.3. Binding Energy Calculation

To determine the binding free energy of the docked complexes, the Prime MM-GBSA integrated with the Prime Schrodinger suite was used [24]. The VSGB solvation system and the OPLS3 force field were used to compute the MMP-9-ligand complexes. The rotamer search technique was also included, along with minimization of the sampling model. The relative free binding energy was computed based on the equation:

$$dGbind = Gcomplex - (Gprotein + Gligand)$$

2.4. Quantum Chemical Calculation

Quantum chemical calculation were performed using Jaguar, a quantum chemistry software integrated into the Maestro platform [25]. The geometry of the molecule was optimized using the B3LYP functional with the 6-31G* basis set. This calculation investigated the highest occupied molecular orbital (HOMO), lowest unoccupied molecular orbital (LUMO), bandgap energy (Eg), ionization potential (I), electron affinity (A), electronegativity (χ), hardness (η), electrophilicity (δ), and the dipole moment (ω) of the compounds using the equations below:

$$Eg = E_{LUMO} - E_{HOMO} \quad (1)$$

$$I = -E_{HOMO} \quad (2)$$

$$A = -E_{LUMO} \quad (3)$$

$$\chi = \frac{I+A}{2} \quad (4)$$

$$\eta = \frac{I-A}{2} \quad (5)$$

$$\delta = \frac{1}{\eta} \quad (6)$$

$$\omega = \frac{\chi 2}{\eta} \quad (7)$$

3. Results

This study employs computational techniques to study the inhibitory potentials of V. vinifera against SARS-CoV-2 Mpro my employing molecular docking, binding energy calculation, ADMET study and quantum chemical calculations. The molecular docking and binding energy calculation was presented in Figure 1, the binding interactions of lead compounds with the amino acid residues present at the active sit of the target was presented in Table 1, ADMET study results were carefully evaluated and presented in Tables 2, 3, 4 and 5.

Table 1. *Binding interactions of lead compounds with the amino acid re.*

Compound	Structure	Interactions
Hyperoside	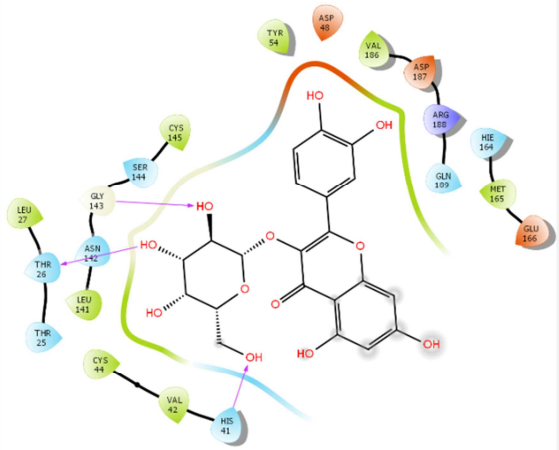	H-Bond Interaction THR 26, GLY 143, HIS 41
Gallocatechin gallate	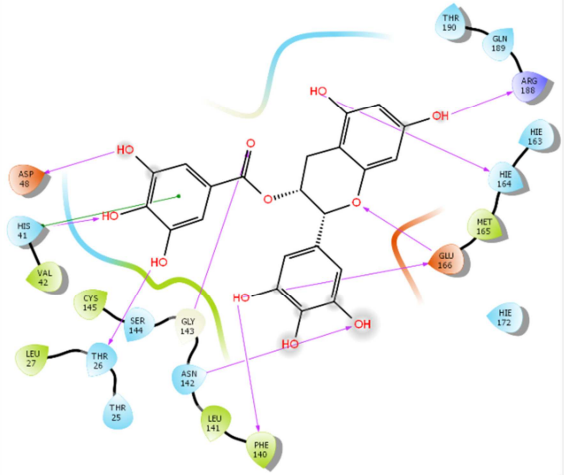	H-Bond Interaction ASP 48, HIS 41, THR 26, GLY 143, ASN 142, PHE 140, GLU 166, HIE 164, ARG 188. Pi-pi cation HIS 41
cis-Astringin	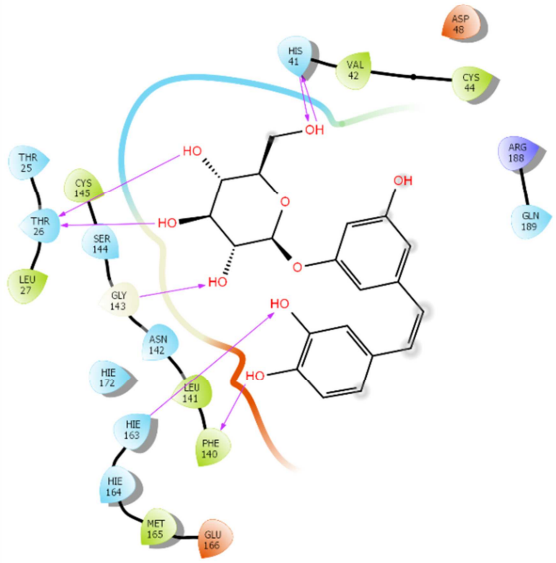	H-Bond Interaction HIS 41, THR 26, GLY 143, HIE 163, PHE 140

Compound	Structure	Interactions
peonidin-3-O-glucoside	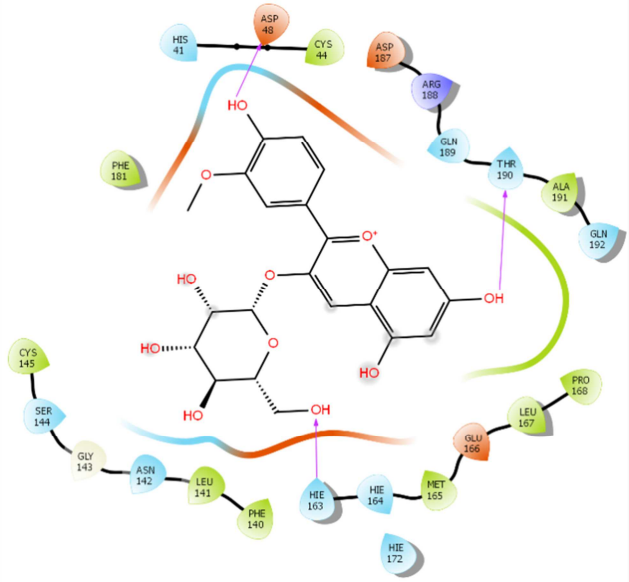	H-Bond Interaction ASP 48, THR 190, HIE 163
Fraxin	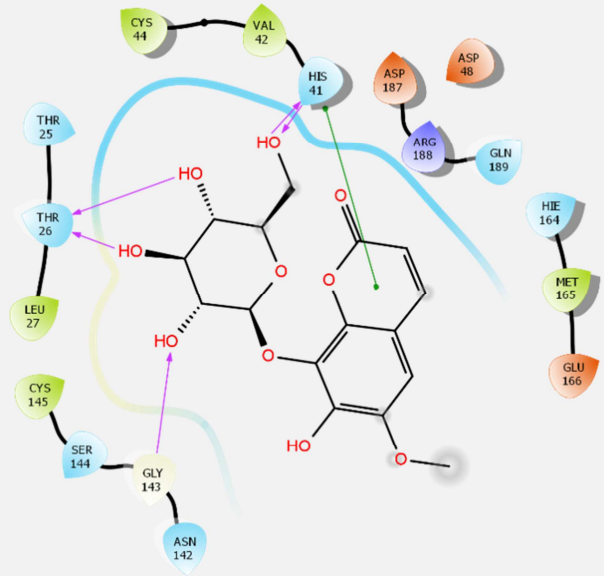	H-Bond Interaction HIS 41, THR 26, GLY 143 Pi-pi cation HIS 41
cis-Piceid	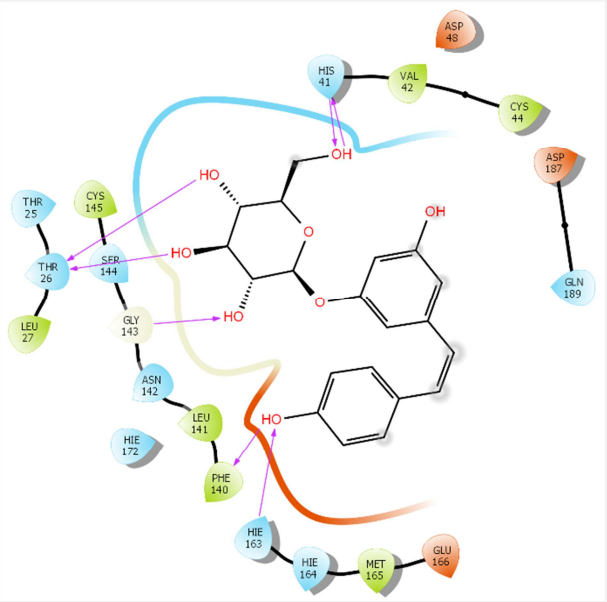	H-Bond Interaction HIS 41, THR 26, GLY 143, PHE 140, HIE 163

Compound	Structure	Interactions
Nelfinavir	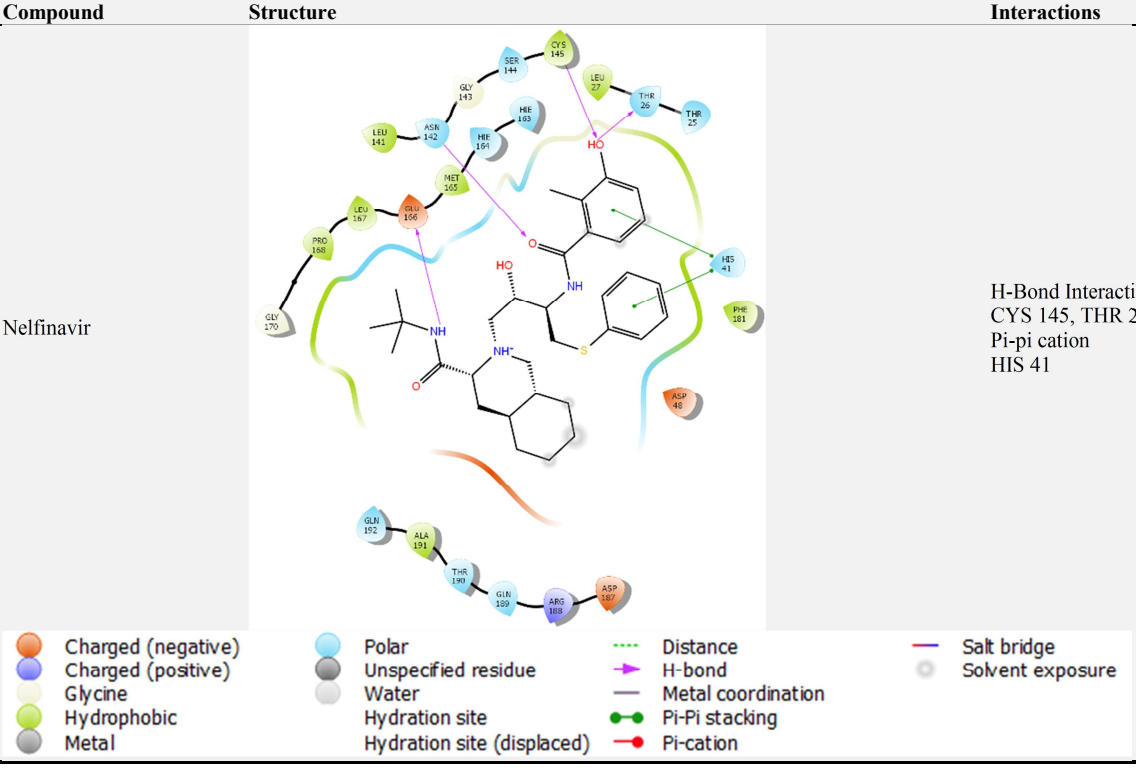	H-Bond Interaction CYS 145, THR 26, ASN 142, GLU 166 Pi-pi cation HIS 41

Table 2. *Lipophilicity (Log P) and water solubility (Log Sw) Prediction with SwissADME.*

Compounds	Consensus Log P	Silicos-IT LogSw	Silicos-IT class
Hyperoside	-0.38	--1.15	Soluble
Gallocatechin gallate	0.99	-2.5	Soluble
Cis-astringin	0.28	-1.02	Soluble
Peonidin-3-o-glucoside	-0.56	-0.93	Soluble
Fraxin	0.57	-1.61	Soluble
Cis-piceid	3.39	-7.26	Poorly soluble
Nelfinavir	-0.77	-1.62	Soluble

Table 3. *Drug-likeness and bioavailability prediction.*

Compounds	Lipinski #violations	Bioavailability score
Hyperoside	2	0.17
Gallocatechin gallate	2	0.17
Cis-astringin	1	0.55
Peonidin-3-o-glucoside	0	0.55
Fraxin	1	0.55
Cis-piceid	1	0.55
Nelfinavir	2	0.17

Table 4. *Pharmacokinetics property prediction.*

Compounds	GI Absorption	BBB permeant	Pgp substrate	CYP1A2 inhibitor	CYP2C59 inhibitor	CYP2C9 inhibitor	CYP2D6 inhibitor	CYP3A4 inhibitor
Hyperoside	Low	No	No	No	No	No	No	No
Gallocatechin gallate	Low	-	-	-	-	-	-	-
Cis-astringin	Low	-	-	-	-	-	-	-
Peonidin-3-o-glucoside	Low	-	-	-	-	-	-	-
Fraxin	High	-	Yes	-	-	-	-	-
Cis-piceid	High	-	Yes	-	Yes	-	-	Yes
Nelfinavir	Low	-	-	-	-	-	-	-

Table 5. *Toxicity prediction by ProTox II.*

Compounds	LD50 (mg/kg)	Toxicity class	Hepatotoxicity	Carcinogenicity	Immunotoxicity	Mutagenicity	Cytotoxicity
Hyperoside	5000	5	-	-	+	-	-
Gallocatechin gallate	1000	4	-	-	-	-	-
Cis-astringin	1380	4	-	-	+	-	-

Compounds	LD50 (mg/kg)	Toxicity class	Hepatotoxicity	Carcinogenicity	Immunotoxicity	Mutagenicity	Cytotoxicity
Peonidin-3-o-glucoside	5000	5	-	-	+	+	-
Fraxin	1380	4	-	-	+	-	-
Cis-piceid	600	4	-	-	+	-	-
Nelfinavir	5000	5	-	-	+	-	+

Table 6. *Quantum chemical calculations of lead compounds compared to the standard compound.*

Compound	HOMO	LUMO	Eg	I	A	χ	η	δ	ω
hyperoside	-0.19954	-0.05785	0.14169	0.19954	0.05785	0.128695	0.070845	14.11532	0.000587
Gallocatechin gallate	-0.21064	-0.03989	0.17075	0.21064	0.03989	0.125265	0.085375	11.71303	0.00067
cis-Astringin	-0.19387	-0.04055	0.15332	0.19387	0.04055	0.11721	0.07666	13.04461	0.000527
peonidin-3-O-glucoside	-0.32995	-0.22887	0.10108	0.32995	0.22887	0.27941	0.05054	19.78631	0.001973
Fraxin	-0.22133	-0.06676	0.15457	0.22133	0.06676	0.144045	0.077285	12.93912	0.000802
cis-Piceid	-0.19707	-0.03899	0.15808	0.19707	0.03899	0.11803	0.07904	12.65182	0.000551
Nelfinavir	-0.29743	-0.11401	0.18342	0.29743	0.11401	0.20572	0.09171	10.90394	0.001941

Table 7. *Representation of the molecular orbitals of lead compounds and the standard compound.*

Compound	HOMO	LUMO
Hyperoside	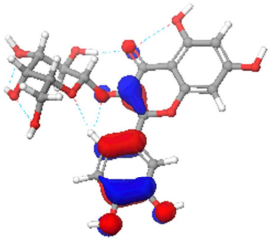	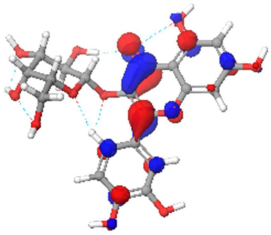
Gallocatechin gallate	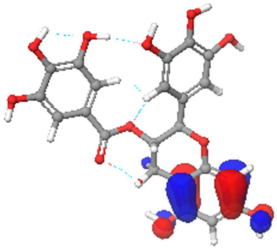	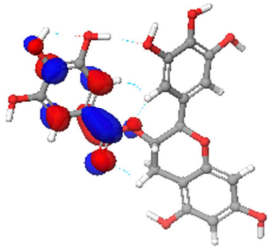
cis-Astringin	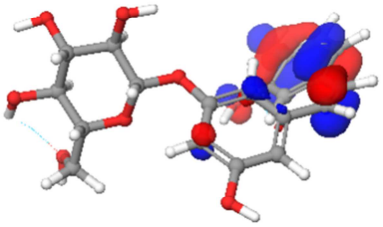	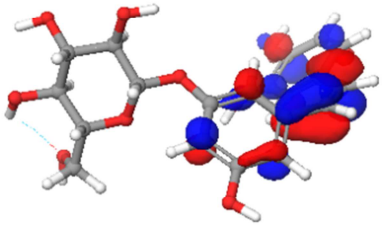
peonidin-3-O-glucoside	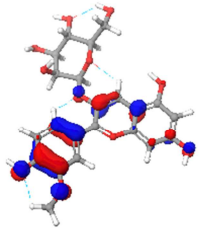	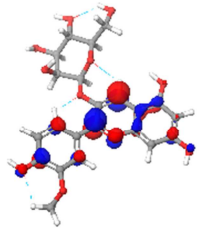
Fraxin	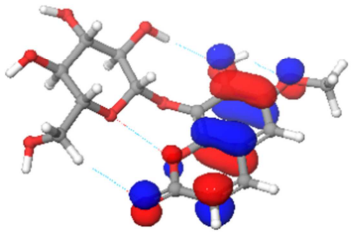	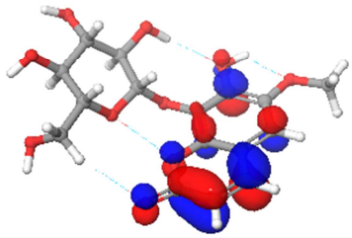

Compound	HOMO	LUMO
cis-Piceid	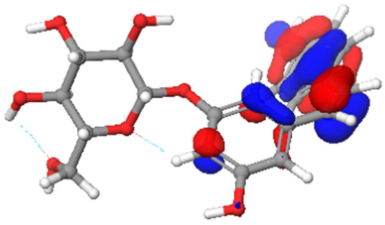	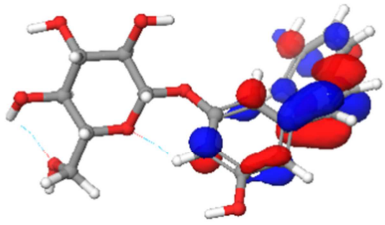
Nelfinavir	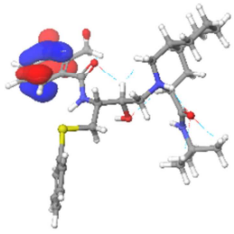	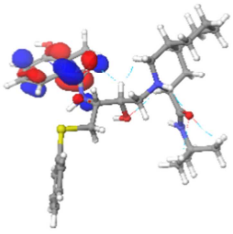

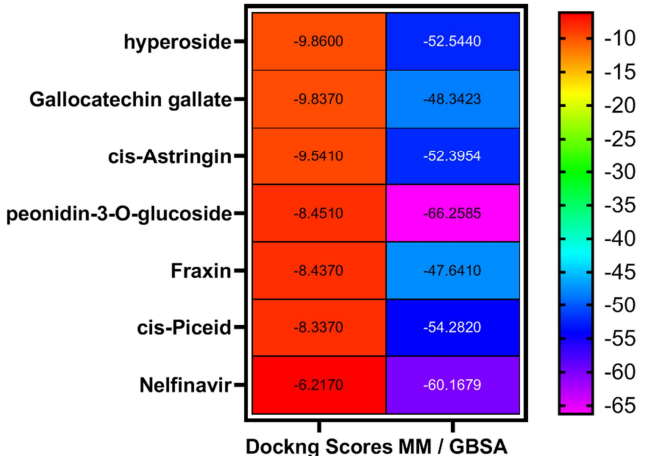

Figure 1. *Heat map showing the docking scores and the binding energies of lead compounds compared with the standard compound.*

4. Discussions

The presented data in Figure 1 represents the molecular docking scores and MMGBSA (Molecular Mechanics Generalized Born Surface Area) dG Bind values for lead compounds after the molecular docking experiment. The lead compounds listed are Hyperoside, Gallocatechin gallate, cis-Astringin, peonidin-3-O-glucoside, Fraxin and cis-Piceid. The affinity and the binding energies of these compounds were compared with a known standard, Nelfinavir.

Docking score represents the predicted binding affinity of a ligand to a protein, with lower scores indicating a stronger binding interaction [26, 27]. From the given data, it was seen that Hyperoside has the lowest docking score of -9.86, suggesting a strong predicted binding affinity to the target protein, followed closely by Gallocatechin gallate with a score of -9.837. cis-Astringin and Fraxin have docking scores of -9.541 and -8.437, respectively, indicating a moderately strong binding affinity. In contrast, cis-Piceid and peonidin-3-O-glucoside have comparatively lower docking scores of -8.337 and -8.451, respectively, suggesting weaker predicted binding interactions. Interestingly, Nelfinavir, a known HIV protease inhibitor [28, 29], has the lowest docking score of -6.217, indicating a weaker predicted binding affinity to the target protein in this case.

The MMGBSA dG Bind value provides an estimation of the free energy of binding between a ligand and a protein [30]. From the results presented in Figure 1, only peonidin-3-O-glucoside was predicted to have a stronger binding energy than the standard compound. This signifies that peonidin-3-O-glucoside has the potential to be stable in the binding cavity of Mpro than Nelfinavir and the remainin compounds. peonidin-3-O-glucoside has a binding energy value of -66.258, Nelfinavir has a binding energy value of -60.167 while the remaining compounds has binding energy values ranging between -47.641 and -54.282.

Interactions are critical in molecular modeling inhibition, as the potency of an inhibitor largely depends on the strength of the binding between a protein and a ligand [31]. The interactions listed in Table 1 represent the specific molecular interactions between each compound and the Mpro. In general, the strength and specificity of these interactions play a crucial role in determining the inhibitory potential of a given compound.

Hydrogen bond was predominantly observed in the results. Pi-pi cation was also observed. In medicinal chemistry, hydrogen bond interactions play a significant role in identifying ligand-target binding and determining target affinity for ligands [27]. Additionally, pi interactions between aromatic rings are crucial in enhancing ligand binding.

Hyperoside exhibited hydrogen bond interactions with three amino acids: THR 26, GLY 143, and HIS 41. Gallocatechin gallate exhibited hydrogen bond interactions with several amino acids, including ASP 48, HIS 41, THR 26, GLY 143, ASN 142, PHE 140, GLU 166, HIE 164, and ARG 188. In addition, this compound also exhibited pi-pi cation interactions with HIS 41. Cis-Astringin exhibited hydrogen bond interactions with HIS 41, THR 26, GLY 143, HIE 163, and PHE 140. Peonidin-3-O-glucoside exhibited hydrogen

bond interactions with ASP 48, THR 190, and HIE 163. Fraxin exhibited hydrogen bond interactions with HIS 41, THR 26, and GLY 143, as well as pi-pi cation interactions with HIS 41. Cis-Piceid exhibited hydrogen bond interactions with HIS 41, THR 26, GLY 143, PHE 140, and HIE 163. Nelfinavir exhibited hydrogen bond interactions with CYS 145, THR 26, ASN 142, and GLU 166, as well as pi-pi cation interactions with HIS 41.

Overall, the presence of hydrogen bond and pi-pi cation interactions suggests that these compounds may have the potential to inhibit the target protein through strong and specific binding.

ADMET study was conducted to probe the physicochemical properties, pharmacokinetic properties, drug-likeness and Toxicity of the lead compounds [32]. The toxicity study was also done for the standard compound to generate a comparative study.

The pharmacokinetic properties of the top-scoring compounds were predicted using SwissAdme and Pro-Tox II.

The structure-based pharmacokinetic screening predicted the values of cardinal pharmacokinetic descriptors such as Lipophilicity, Water Solubility and oral bioavailability score among others. Specifically, consensus Log P, an average of five predictive models of lipid solubility was employed to characterize the lipophilic behavior of the test compounds. Technically, the lipophilic behavior of compounds is measure computationally as the partition coefficient of n-octanol to water. The results showed that cis-piceid exhibited the highest lipophilicity of all compounds tested with a Log P value of of 3.39. Compounds that are projected as drug candidates require an optimal level of lipid solubility to enable their movement across membranes. This is specifically required for their absorption across the lumen of the small intestine and their deposition into target cells. Other compounds had much lower lipophilic behaviors. gallocatechin gallate, fraxin, and cis-astringin returned values of 0.99, 0.57, and 0.28 respectively. Meanwhile, hyperoside, peonidin-3-o-glucoside and nelfinavir had negative values of -0.38, -0.56, and -0.77 respectively. Despite the crucuiality of lipid solubility, optimal water solubility is equally important for compounds that are projected as drug molecules to aid systemic circulation of the compounds. According to the result in Table 2. hyperoside to fraxin and nelfinavir are predicted to be soluble in water while fraxin is predicted to be poorly soluble.

The Lipinski's Rule of Five, also known as the "Rule of Five," is a guideline for determining whether a compound is likely to be orally bioavailable, which means that it can be absorbed into the bloodstream after being taken orally [33]. The rule is based on four physicochemical properties of a compound: molecular weight, lipophilicity (measured by Log P), hydrogen bond donors, and hydrogen bond acceptors [33]. According to table 3, hyperoside, gallocatechin gallate and nelfinavir violates only 2 rules each of the Lipinski rules, cis-astringin, fraxin and cis-piceid violates 1 rule each and peonidin-3-o-glucoside did not violate any rule. The violation by all the compounds is generally acceptable.

Bioavailability is a measure of the fraction of an administered dose of a drug that reaches the systemic circulation in an unchanged form [34]. hyperoside, gallocatechin gallate and nelfinavir has a bioavailability of 0.17 while cis-astringin to cis-piceid has 0.55. A bioavailability score of 0.55 means that 17% of the administered dose of the compound reaches the systemic circulation in an unchanged form, while the remaining 83% may be metabolized, excreted, or otherwise eliminated from the body before reaching the systemic circulation. This also applies to the compounds with 0.55 bioavailability score. This signifies that most of the lead compounds possess better bioavailability than the standard compound.

Predicting the pharmacokinetics of a drug candidate is important in drug discovery and development as it can help to identify potential issues with a drug candidate early in the development process [35]. The Pharmacokinetic properties of the lead compound were evaluated and it was discovered.

Table 4 contains information about the pharmacokinetic properties of the lead compounds, including their GI absorption, BBB permeability, Pgp substrate status, and their ability to inhibit various cytochrome P450 (CYP) enzymes, as well as their log Kp values.

GI absorption refers to the ability of a drug to be absorbed from the gastrointestinal tract into the bloodstream [36]. Compounds hyperoside-peonidin-3-o-glucoside have low GI absorption, meaning that they may not be efficiently absorbed and may require a larger dose or a different route of administration. Compounds fraxin and nelfinavir, on the other hand, have high GI absorption, which suggests that they can be efficiently absorbed from the GI tract. BBB permeability refers to the ability of a compound to cross the blood-brain barrier (BBB). The BBB is a specialized barrier that separates the central nervous system (CNS) from the bloodstream and regulates the passage of substances into the brain [37]. None of the compouds were predicted to be able to cross the BBB. P-glycoprotein (Pgp) is a transporter protein that is involved in the efflux of drugs and other substances from cells. Only fraxin and cis-piceid were predicted to be Pgp substrate. The cytochrome P450 (CYP) enzymes are involved in the metabolism of many drugs. Inhibition of CYP enzymes can lead to increased plasma concentrations of drugs and potentially increase the risk of adverse effects or drug interactions. Compounds hyperoside to fraxin and nelfinavir are not inhibitors of any of the CYP enzymes tested. Compounds cis-piceid was predicted to be inhibitors of CYP2C59 and CYP3A4.

Table 5 provides information on the toxicity of the lead compounds compared to the standard compound, based on their LD50 (lethal dose 50%) values and various types of toxicity.

LD50 is a measure of the acute toxicity of a substance, indicating the dose required to cause death in 50% of the animals exposed to it [38]. The lower the LD50, the more toxic the substance is considered to be. According to table 5, the LD50 values range from 600 mg/kg to 5000 mg/kg, with compounds hyperoside, peonidin-3-o-glucoside, and

nelfinavir having an LD50 of 5000 mg/kg, which suggests they are less toxic than the other compounds. cis-astringin and fraxin has LD50 of 1380 mg/kg, while compounds gallocatechin gallate have LD50 of 1000 mg/kg and compounds cis-piceid have LD50 of 600 mg/kg, indicating that they are more toxic.

The toxicity class is a classification system used to indicate the level of toxicity of a substance. In this case, the toxicity classes range from 1 (highly toxic) to 5 (relatively non-toxic). According to Table 5, compounds hyperoside, peonidin-3-o-glucoside, and nelfinavir have a toxicity class of 5, indicating that they are relatively non-toxic. Compounds gallocatechin gallate, cis-astringin, and fraxin have a toxicity class of 4, indicating a low to moderate level of toxicity.

The table also provides information on various types of toxicity, including hepatotoxicity, carcinogenicity, immunotoxicity, mutagenicity, and cytotoxicity. None of the compounds are known to be carcinogenic or hepatotoxic. However, only gallocatechin gallate is predicted not to be immunotoxic. Likewise, only compounds peonidin-3-o-glucoside was predicted to be cytotoxic and only nelfinavir was predicted to be mutagenic.

Quantum chemical studies provide insight into the chemical activities and stability of compounds, primarily through analysis of frontier molecular orbitals (FMOs), such as the highest occupied molecular orbital (HOMO) and the lowest unoccupied molecular orbital (LUMO) [39, 40] (as shown in Table 7), which relate to electron affinity and ionization potential [41], respectively. These orbitals are used to investigate the electronic properties of compounds and to understand their chemical stability and reactivity [42]. In this study, the energetic behaviors and reactivity of selected compounds against the COVID-19 virus were determined by analyzing the FMOs, electronic transitions, and energy differences through EHOMO and ELUMO (Eg) [43]. The results are presented in Table 6, along with their reactivity descriptors.

The HOMO is where the highest energy and electrons for donation are located, while the LUMO identifies compounds that are available to accept electrons. The HOMO-LUMO band gap (Eg) can be used to determine the most reactive compound [44, 45]; a smaller band gap indicates higher reactivity, as less energy is required to promote an electron from the HOMO to the LUMO [46]. Peonidin-3-O-glucoside has the smallest band gap (Eg = 0.10108 eV) and is expected to be the most reactive compound.

The ionization potential of a molecule determines its ability to donate electrons and become positively charged, while the electron affinity indicates its tendency to accept electrons and become negatively charged [47]. According to Table 2, compounds with higher HOMO energies (Nelfinavir and Peonidin-3-O-glucoside) are less likely to donate electrons, while those with higher LUMO energies (Fraxin and Peonidin-3-O-glucoside) are more likely to accept electrons [48]. This is consistent with the ionization potential and electron affinity values in Table 2. Peonidin-3-O-glucoside, however, is only identified as a compound with a higher tendency to accept electrons because of its higher electron affinity. This can be attributed to the oxygen species deficiency on the pyran substituent [45], as seen in Figure 1, which shifts the LUMO towards it.

The electronegativity (χ) values suggest that the compounds are moderately polar, with values ranging from 0.118 to 0.279. Peonidin-3-O-glucoside has the highest electronegativity value, indicating that it is the most polar of all the studied compounds.

The chemical hardness (η) and softness (δ) values suggest that the studied compounds are relatively hard, which means that they are less likely to undergo chemical reactions. Peonidin-3-O-glucoside has the highest hardness value, which is consistent with its high ionization potential and electron affinity values. The dipole moment (V) values suggest that the studied compounds are moderately polar, with values ranging from 0.000551 to 0.001973. Peonidin-3-O-glucoside has the highest dipole moment value, indicating that it is the most polar of all the studied compounds.

5. Conclusion

This research utilized molecular docking, binding energy calculation, ADMET study, and quantum chemical calculations to model potential SARS-CoV-2 Mpro inhibitors from *V. Vinifera* extracts. Six compounds, including Hyperoside, Gallocatechin gallate, cis-Astringin, peonidin-3-O-glucoside, Fraxin, and cis-Piceid, were identified as having the potential to inhibit SARS-CoV-2 Mpro. When compared to the known standard Nelfinavir, these compounds showed better binding affinities and slightly improved ADMET properties. Particularly, peonidin-3-O-glucoside exhibited better binding energy, reactivity, and stability than the other compounds and the standard, suggesting that it may have potential as an inhibitor of SARS-CoV-2 Mpro. Nevertheless, additional in vivo and in vitro studies are required to validate these findings.

References

[1] Oyagbemi AA, Ajibade TO, Aboua YG, Gbadamosi IT, Adedapo ADA, Aro AO, et al. Potential health benefits of zinc supplementation for the management of COVID-19 pandemic. Journal of Food Biochemistry. 2021; 45 (2): e13604.

[2] WHO Coronavirus (COVID-19) Dashboard [Internet]. [cited 2023 May 4]. Available from: https://covid19.who.int

[3] Transmissibility and transmission of respiratory viruses | Nature Reviews Microbiology [Internet]. [cited 2023 May 4]. Available from: https://www.nature.com/articles/s41579-021-00535-6

[4] Shi Y, Wang G, Cai X peng, Deng J wen, Zheng L, Zhu H hong, et al. An overview of COVID-19. Journal of Zhejiang University Science B. 2020 May; 21 (5): 343.

[5] Hoofman J, Secord E. The Effect of COVID-19 on Education. Pediatric Clinics. 2021 Oct 1; 68 (5): 1071–9.

[6] The Economic Effects of COVID-19 Containment Measures | SpringerLink [Internet]. [cited 2023 Apr 25]. Available from: https://link.springer.com/article/10.1007/s11079-021-09638-2

[7] Targeting SARS-CoV-2 Main Protease for Treatment of COVID-19: Covalent Inhibitors Structure–Activity Relationship Insights and Evolution Perspectives | Journal of Medicinal Chemistry [Internet]. [cited 2023 May 4]. Available from: https://pubs.acs.org/doi/full/10.1021/acs.jmedchem.2c01005

[8] Mujwar S, Harwansh RK. In silico bioprospecting of taraxerol as a main protease inhibitor of SARS-CoV-2 to develop therapy against COVID-19. Struct Chem. 2022/05/04 ed. 2022 Apr 28; 1–12.

[9] Johnson TO, Adegboyega AE, Ojo OA, Yusuf AJ, Iwaloye O, Ugwah-Oguejiofor CJ, et al. A Computational Approach to Elucidate the Interactions of Chemicals From Artemisia annua Targeted Toward SARS-CoV-2 Main Protease Inhibition for COVID-19 Treatment. Front Med (Lausanne). 2022 Jun 15; 9: 907583.

[10] Akinnusi PA, Olubode SO, Salaudeen WA. Molecular binding studies of anthocyanins with multiple antiviral activities against SARS-CoV-2. Bull Natl Res Cent. 2022 Dec; 46 (1): 102.

[11] Adebesin AO, Ayodele AO, Omotoso O, Akinnusi PA, Olubode SO. Computational evaluation of bioactive compounds from *V. Vinifera* as a novel β-catenin inhibitor for cancer treatment. Bull Natl Res Cent. 2022 Dec; 46 (1): 183.

[12] Olubode SO, Bankole MO, Akinnusi PA, Adanlawo OS, Ojubola KI, Nwankwo DO, et al. Molecular Modeling Studies of Natural Inhibitors of Androgen Signaling in Prostate Cancer. Cancer Inform. 2022 Jan; 21: 117693512211185.

[13] Bongo GN, Ngbolua KTN, Mbadiko Mutunda C, Inkoto C, Mpiana PT, Gbolo BZ, et al. Phytochemistry and Antiviral activities of some fruit plant species as potential resources for anti-viral agents: A review. 2022 Mar 11; 3: 1–11.

[14] Olubode S, Bankole O, Akinnusi P, Salaudeen W, Ojubola K, Adanlawo O, et al. Computational study of the inhibitory potential of Gongronema latifolium (benth) leave on farnesyl pyrophosphate synthase, a target enzyme in the treatment of osteoporosis. A molecular modelling approach. Journal of Herbal Drugs. 2022; 13 (2): 10.

[15] Olubode SO, I Omotuyi O, Fadipe D. Computational Prediction of HCV RNA Polymerase Inhibitors from Alkaloid Library. Lett Appl NanoBioSci. 2021 Sep 7; 11 (3): 3661–71.

[16] Friesner RA, Murphy RB, Repasky MP, Frye LL, Greenwood JR, Halgren TA, et al. Extra Precision Glide: Docking and Scoring Incorporating a Model of Hydrophobic Enclosure for Protein−Ligand Complexes. J Med Chem. 2006 Oct 1; 49 (21): 6177–96.

[17] Kim S, Thiessen PA, Bolton EE, Chen J, Fu G, Gindulyte A, et al. PubChem Substance and Compound databases. Nucleic Acids Res. 2016 Jan 4; 44 (D1): D1202–13.

[18] Release S. LigPrep, Schrödinger, LLC, New York, NY, 2017. New York, NY.

[19] Bissantz C, Folkers G, Rognan D. Protein-Based Virtual Screening of Chemical Databases. 1. Evaluation of Different Docking/Scoring Combinations. J Med Chem. 2000 Dec 1; 43 (25): 4759–67.

[20] Harder E, Damm W, Maple J, Wu C, Reboul M, Xiang JY, et al. OPLS3: A Force Field Providing Broad Coverage of Drug-like Small Molecules and Proteins. J Chem Theory Comput. 2016 Jan 12; 12 (1): 281–96.

[21] Glide Docking, Autodock, Binding Free Energy and Drug-Likeness Studies for Prediction of Potential Inhibitors of Cyclin-Dependent Kinase 14 Protein in Wnt Signaling Pathway. Biointerface Res Appl Chem. 2021 Jun 18; 12 (2): 2473–88.

[22] Daina A, Michielin O, Zoete V. SwissADME: a free web tool to evaluate pharmacokinetics, drug-likeness and medicinal chemistry friendliness of small molecules. Sci Rep. 2017 May 12; 7 (1): 42717.

[23] Banerjee P, Eckert AO, Schrey AK, Preissner R. ProTox-II: a webserver for the prediction of toxicity of chemicals. Nucleic Acids Research. 2018 Jul 2; 46 (W1): W257–63.

[24] Jacobson MP, Friesner RA, Xiang Z, Honig B. On the Role of the Crystal Environment in Determining Protein Side-chain Conformations. Journal of Molecular Biology. 2002 Jul; 320 (3): 597–608.

[25] Jaguar: A high-performance quantum chemistry software program with strengths in life and materials sciences - Bochevarov - 2013 - International Journal of Quantum Chemistry - Wiley Online Library [Internet]. [cited 2023 May 4]. Available from: https://onlinelibrary.wiley.com/doi/full/10.1002/qua.24481

[26] K Inyang O, I Omotuyi O, J Ogunleye A, O Eniafe G, Adewumi B, S Metibemu D. Molecular Interaction and Inhibitory Potential of Polyphenol on DNA Repair Pathway in Small Cell Lung Cancer: A Computational Study. JAPLR [Internet]. 2017 Oct 25 [cited 2022 Jun 24]; 6 (3). Available from: https://medcraveonline.com/JAPLR/molecular-interaction-and-inhibitory-potential-of-polyphenol-on-dna-repair-pathway-in-small-cell-lung-cancer-a-computational-study.html

[27] Akinnusi PA, Olubode SO, Alade AA, Ahmed SA, Ayekolu SF, Ogunlade TM, et al. A molecular modeling approach for structure-based virtual screening and identification of novel anti-hypercholesterolemic agents from Grape. Informatics in Medicine Unlocked. 2022; 32: 101065.

[28] Ray AK, Sen Gupta PS, Panda SK, Biswal S, Bhattacharya U, Rana MK. Repurposing of FDA-approved drugs as potential inhibitors of the SARS-CoV-2 main protease: Molecular insights into improved therapeutic discovery. Computers in Biology and Medicine. 2022 Mar 1; 142: 105183.

[29] Avti P, Chauhan A, Shekhar N, Prajapat M, Sarma P, Kaur H, et al. Computational basis of SARS-CoV 2 main protease inhibition: an insight from molecular dynamics simulation based findings. Journal of Biomolecular Structure and Dynamics. 2022 Nov 26; 40 (19): 8894–904.

[30] Akinnusi PA, Olubode SO, Adebesin AO, Osadipe TJ, Nwankwo DO, Adebisi AD, et al. Structure-based scoring of anthocyanins and molecular modeling of PfLDH, PfDHODH, and PfDHFR reveal novel potential P. falciparum inhibitors. Informatics in Medicine Unlocked. 2023 Jan 1; 38: 101206.

[31] Akinnusi PA, Olubode SO, Adebesin AO, Nana TA, Shodehinde SA. Discovery of Promising Inhibitors of Epidermal Growth Factor Receptor (EGFR), Human Epidermal Growth Factor Receptor 2 (HER2), Estrogen Receptor (ER), and Phosphatidylinositol-3-kinase a (PI3Ka) for Personalized Breast Cancer Treatment. Cancer Inform. 2022 Jan; 21: 117693512211278.

[32] Omoboyowa DA, Balogun TA, Saibu OA, Chukwudozie OS, Alausa A, Olubode SO, et al. Structure-based discovery of selective CYP17A1 inhibitors for Castration-resistant prostate cancer treatment. Biology Methods and Protocols. 2022 Jan 10; 7 (1): bpab026.

[33] Lipinski CA. Lead- and drug-like compounds: the rule-of-five revolution. Drug Discovery Today: Technologies. 2004 Dec; 1 (4): 337–41.

[34] Optometric Management - April 2022 [Internet]. Optometric Management. [cited 2023 May 4]. Available from: https://www.optometricmanagement.com/newsletters/nutritional-insights-for-clinical-practice/april-2022

[35] Recent Advances in the Prediction of Pharmacokinetics Properties in Drug Design Studies: A Review - Pantaleão - 2022 - ChemMedChem - Wiley Online Library [Internet]. [cited 2023 May 4]. Available from: https://chemistry-europe.onlinelibrary.wiley.com/doi/abs/10.1002/cmdc.202100542

[36] Wilson CG, Aarons L, Augustijns P, Brouwers J, Darwich AS, De Waal T, et al. Integration of advanced methods and models to study drug absorption and related processes: An UNGAP perspective. European Journal of Pharmaceutical Sciences. 2022 May 1; 172: 106100.

[37] Teleanu RI, Preda MD, Niculescu AG, Vladâcenco O, Radu CI, Grumezescu AM, et al. Current Strategies to Enhance Delivery of Drugs across the Blood–Brain Barrier. Pharmaceutics. 2022 May; 14 (5): 987.

[38] Zwickl CM, Graham JC, Jolly RA, Bassan A, Ahlberg E, Amberg A, et al. Principles and procedures for assessment of acute toxicity incorporating in silico methods. Computational Toxicology. 2022 Nov 1; 24: 100237.

[39] Noureddine O, Issaoui N, Medimagh M, Al-Dossary O, Marouani H. Quantum chemical studies on molecular structure, AIM, ELF, RDG and antiviral activities of hybrid hydroxychloroquine in the treatment of COVID-19: Molecular docking and DFT calculations. Journal of King Saud University - Science. 2021 Mar 1; 33 (2): 101334.

[40] Silva R, Santos J, Figueroa-Villar J. On the Limits of Highest-Occupied Molecular Orbital Driven Reactions: The Frontier Effective-for-Reaction Molecular Orbital Concept. The journal of physical chemistry A. 2006 Feb 1; 110: 1031–40.

[41] Louis E, San-Fabián E, Díaz-García MA, Chiappe G, Vergés JA. Are Electron Affinity and Ionization Potential Intrinsic Parameters to Predict the Electron or Hole Acceptor Character of Amorphous Molecular Materials? J Phys Chem Lett. 2017 Jun 1; 8 (11): 2445–9.

[42] Mumit MA, Pal TK, Alam MA, Islam MAAAA, Paul S, Sheikh MC. DFT studies on vibrational and electronic spectra, HOMO–LUMO, MEP, HOMA, NBO and molecular docking analysis of benzyl-3-N-(2, 4, 5-trimethoxyphenylmethylene) hydrazinecarbodithioate. J Mol Struct. 2020 Nov 15; 1220: 128715.

[43] Mohapatra R, Mohapatra P, Azam M, Sarangi A, Abdalla M, Perekhoda L, et al. Computational studies on potential new anti-Covid-19 agents with a multi-target mode of action. Journal of King Saud University - Science. 2022 May 10; 34.

[44] Huang Y, Rong C, Zhang R, Liu S. Evaluating frontier orbital energy and HOMO/LUMO gap with descriptors from density functional reactivity theory. Journal of Molecular Modeling. 2017 Jan 1; 23.

[45] Sens L, Oliveira A, Mascarello A, Brighente II, Yunes R, Nunes R. Synthesis, Antioxidant Activity, Acetylcholinesterase Inhibition and Quantum Studies of Thiosemicarbazones. Journal of the Brazilian Chemical Society. 2017 Jan 1; 29.

[46] Pegu D, Deb J, Van Alsenoy C, Sarkar U. Theoretical Investigation of Electronic, Vibrational and Nonlinear Optical Properties of 4-fluoro-4-hydroxybenzophenone. Spectroscopy Letters. 2017 Mar 22; 50.

[47] El-Shamy NT, Alkaoud AM, Hussein RK, Ibrahim MA, Alhamzani AG, Abou-Krisha MM. DFT, ADMET and Molecular Docking Investigations for the Antimicrobial Activity of 6, 6′-Diamino-1, 1′, 3, 3′-tetramethyl-5, 5′-(4-chlorobenzylidene) bis[pyrimidine-2, 4 (1H, 3H)-dione]. Molecules. 2022 Jan 18; 27 (3): 620.

[48] Miar M, Shiroudi A, Pourshamsian K, Oliaey AR, Hatamjafari F. Theoretical investigations on the HOMO–LUMO gap and global reactivity descriptor studies, natural bond orbital, and nucleus-independent chemical shifts analyses of 3-phenylbenzo[d] thiazole-2 (3H)-imine and its para-substituted derivatives: Solvent and substituent effects. Journal of Chemical Research. 2021 Jan 1; 45 (1–2): 147–58.